Asian Journal of Chemistry; Vol. 33, No. 7 (2021), 1513-1518

ASIAN JOURNAL OF CHEMISTRY

https://doi.org/10.14233/ajchem.2021.23193

Analogy and Comparative Study of Hydroxypropyl Methylcellulose (HPMC) Biopolymer with Graphene Oxide and Zinc Oxide Nano Fillers

SANOOP PADINHATTAYIL* and K. SHESHAPPA RAI

Department of Post-Graduate Studies and Research in Polymer Science, University of Mysore, Sir M. Visvesvaraya Post-Graduate Centre, Tubinakere, Mandya-571402, India

*Corresponding author: E-mail: sanoop.home@gmail.com

Received: 5 March 2021; *Accepted*: 12 April 2021; *Published online*: 26 June 2021; AJC-20390

Present study describes the analogy and comparative study of polymer nanocomposites with the known polymer matrix hydroxypropyl methylcellulose (HPMC) incorporated with graphene oxide (GO) and zinc oxide (ZnO) nanoparticles as nano fillers. The polymer nanocomposite films were carried out using solution casting method and characterized by IR spectroscopy, XRD analysis, mechanical properties, thermal characterization and optical microscopy analysis. There were several changes in the HPMC polymer by the addition of nanoparticles of GO and ZnO in structural, thermal, mechanical and optical properties. The thermal stability of the composite films increased as compared with the pure HPMC whereas the mechanical study shows a variation of down values.

Keywords: Hydroxypropyl methylcellulose, Nanocomposites, Zinc oxide, Graphene oxide, Band gap.

INTRODUCTION

Polymer nanocomposite production has progressed rapidly because, due to improved thermal stability, light in weight than that of pure polymers and polymer composite materials. To prepare these materials, several natural polymers, synthetic polymers, biopolymers and elastomers can be used, comprising, depending on the application, various nanoparticles integrated into them [1-9]. It is important to select the right polymer-nanoparticle combination and processing technique to analyze these novel materials with good specifications, since the new design relies on this. In order to understand the behaviour of new materials, the following essential facts on components must be considered for the manufacture of polymer nanocomposites: (i) polymer mass; (ii) polymer chemical structure; (iii) polymer semi-crystalline; (iv) polymer mass; (v) polymer composition; (vi) polymer semi-crystallinity; (vii) thermal resilience of the polymer; (viii) surface area of the nanoparticle; (ix) chemical composition of the nanoparticle; and (x) dispersion of the nanoparticle. To extract these materials, there are many processes, the most prominent to be *in situ* polymerization, dispersion of solutions (including nano precipitation and spray drying) and extrusion of melt. Each method has a uniqueness of its own. However, regardless of the method, the nature among all polymer nanocomposites is the final morphology, which relies on polymer-nanoparticle interactions that facilitate uniform dispersion and deposition of the nanoparticles with polymer matrix [10-14].

As long as their properties could be adapted to particular end-use applications, biopolymers, such as cellulose and its derivatives, can provide attractive alternatives. Hydroxypropyl methylcellulose (HPMC) is among the most widely applied cellulose ethers in the food industry as an emulsifier, defensive colloid, stabilizing agent, suspension agent, thickener agent, including film former, *etc*. [15]. Due of their specific physical and chemical characteristics, zinc oxide nanoparticles is an eco-friendly substance with no toxicity [16,17] and one of the multipurpose inorganic nanoparticles, which favours the bio-applications [18]. Moreover, ZnO nanoparticles are also used in the rubber industry and provide rubber wear resistance, enhancing high polymer efficiency in their strength, intensity, anti-aging and other features [19,20]. Due to the simplicity, cost-effective, durability, consistency and relatively mild conditions of the system′s development, ZnO nanopowders produced mostly by sol-gel approach have attracted considerable attention. This technique enables the surface modification of zinc oxide

with appropriate organic material compounds which influence the properties of particles and widen their application spectrum.

The monolayer of hexagonally packed carbon atoms, graphene, has essentially revolutionized both the academic and industrial fields [21]. Its novel characteristics such as high modulus and tensile strength, large theoretical real surface area, practically transparent and superior conductivity, could be of quite great relevance among these potential ones. Due to the combined enhanced properties, functionalized graphene as well as its composites, polymer-based graphene composites are very potential material [22]. For many practical uses in large-scale processing, graphene is commonly used as a nano filler in polymer composites. The intense interaction produced between graphene oxide polar molecules is due to the effects of functional groups containing oxygen to have homogeneous dispersion [23]. Due to its thermal stability [24], mechanical strength [25] and enhanced ionic conductivity [26], graphene oxide doped polymer nanocomposite films have been reported.

In this work, the effects of ZnO and GO nanoparticles on the structural, mechanical and thermal properties of HPMC films are studied. To maximize the efficiency of the composites obtained, different concentrations of nanoparticles have also been examined.

EXPERIMENTAL

All chemicals used in this study were of analytical grade. HPMC was purchased from CDH, India with a molecular weight of 120000 Dalton. Graphite flakes with particle size 60 meshes were obtained from Loba Chemie. Zinc sulphate, zinc acetate dihydrate, sodium hydroxide, sulfuric acid, hydrochloric acid, ethanol hydrogen peroxide, potassium permanganate and sodium nitrate were procured from S.D. Fine Chemicals, India. Double distilled water was used for the preparation of composite films.

Preparation of HPMC/ZnO and HPMC/GO nanocomposites: The ZnO nanoparticles were extracted using a controlled method of precipitation. A dropwise molar ratio of 1:2 has been introduced to the aqueous solution of zinc sulphate and sodium hydroxide under intense stirring for almost 12 h. The acquired precipitate was filtered, washed with deionized water then dried in hot air oven at 100 ºC. The powder collected became calcinated inside a muffle furnace over 2 h at 550 ºC. The obtained ZnO nanoparticles were characterized by XRD and FTIR.

From the modified Hummer Process, GO was prepared [27,28] and characterized by X-ray diffraction (XRD) and Fourier transmission infrared (FTIR) to confirm the average nano size and the structure, respectively [27].

The method of solution casting has been used for the development of nanocomposite films. HPMC (4% w/w) was dissolved in double distilled water at room temperature. To separate HPMC solution, added ZnO and GO nanoparticles with varying concentrations as weight percent of 1, 3 and 5. The mixture was held for 5-6 h in a stirring mode. To homogenize, the sonicator was used for 10 min, then the solution was poured into petri dishes for uniform thickness and finally dried in air.

Characterization techniques: The crystal structures for nanocomposite films were tested through using techniques as XRD (XPERT-MPD diffractometer). Using the X-ray diffractometer (radiation Cu$K\alpha$ and λ = 0.15406 nm), the patterns were taken. The intensity was calculated in the scanning rate of 10º/min along with 2θ range of 10-70º. To indentify, the chemical bonding between samples, the FTIR spectrophotometer in the range of wavelength of 4000-500 cm^{-1} had been used. Scanning electron microscopy (SEM) analyzed the morphology of ZnO nanoparticles as well as the film surface. In compliance with ASTM Standard Process D882-02 (ASTM, 2002), the mechanical properties of the samples, including tensile strength (TS), elongation and Young′s module at the break were tested using the Universal testing machine. The experiments were conducted with three replications.

RESULTS AND DISCUSSION

XRD analysis: The nanocomposites of pure HPMC and HPMC/GO exhibit two diffraction peaks at 10.23º and 25.80º which indicate the peaks for GO and the 2θ value for the HPMC peak remains the same in all compositions of nanocomposites (Fig. 1). The formation of well-exfoliated GO/HPMC nanocomposites was determined and it can be seen that the nature of HPMC remains unchanged even after GO is implanted into the HPMC matrix.

The XRD patterns of HPMC pure film and HPMC/ZnO nanocomposite films with varying concentrations of ZnO are presented in Fig. 2. The XRD pattern of pure HPMC (Fig. 1) confirmed that HPMC is an amorphous polymer [29] with a single large peak at 2θ = 20.21º. Due to very low concentration, the intensity of ZnO peaks was not traced on 1% and 3% loading of nanoparticles in the HPMC network. The ZnO peaks were observed in 5% loading at 2θ =31.85º and 2θ =36.17º, which confirms the presence of ZnO nanoparticles [27] in the HPMC polymer matrix.

FTIR analysis: The FT-IR spectrum of HPMC/ZnO nanocomposite films is shown in Fig. 3. The samples revealed that the peaks at 3429.45 cm^{-1} are responsible for the OH stretching vibration and intermolecular H-bonding [30]. The peak at 2918.95 cm^{-1} corresponds to CH stretching vibration and the band at 1645.46 cm^{-1} indicate the existence of ν(C-O) six-membered cyclic rings of stretching vibration. The methoxy group′s symmetric bending vibrations are seen in between 1400-1350 cm^{-1} range [31]. Moreover, the band at 1052.35 cm^{-1} is due to the stretching vibration of C-O groups.

In the FTIR spectra of HPMC/GO, the O-H stretching is allocated to the peak at 3429.30 cm^{-1} and caused by the presence of a significant number of hydroxyl groups in the backbone of GO [32]. The various signature bands responsible for the different functionalities of oxygen found in the GO. The band at 1645.65 cm^{-1} is part of the carbonyl residue (C=O) stretching vibration, while the peak at 1412.20 cm^{-1} is attributed to the carboxyl group in GO. The skeletal vibration from non-oxidized graphitic peaks at 1645.45 cm^{-1} is the characteristic band. The the absorbance bands at 1267 and 1053.30 cm^{-1} are due to the epoxy and alkoxy groups, respectively [33]. All of these results confirmed the eventual formation of ZnO and GO nanoparticles in the HPMC matrix in every composition.

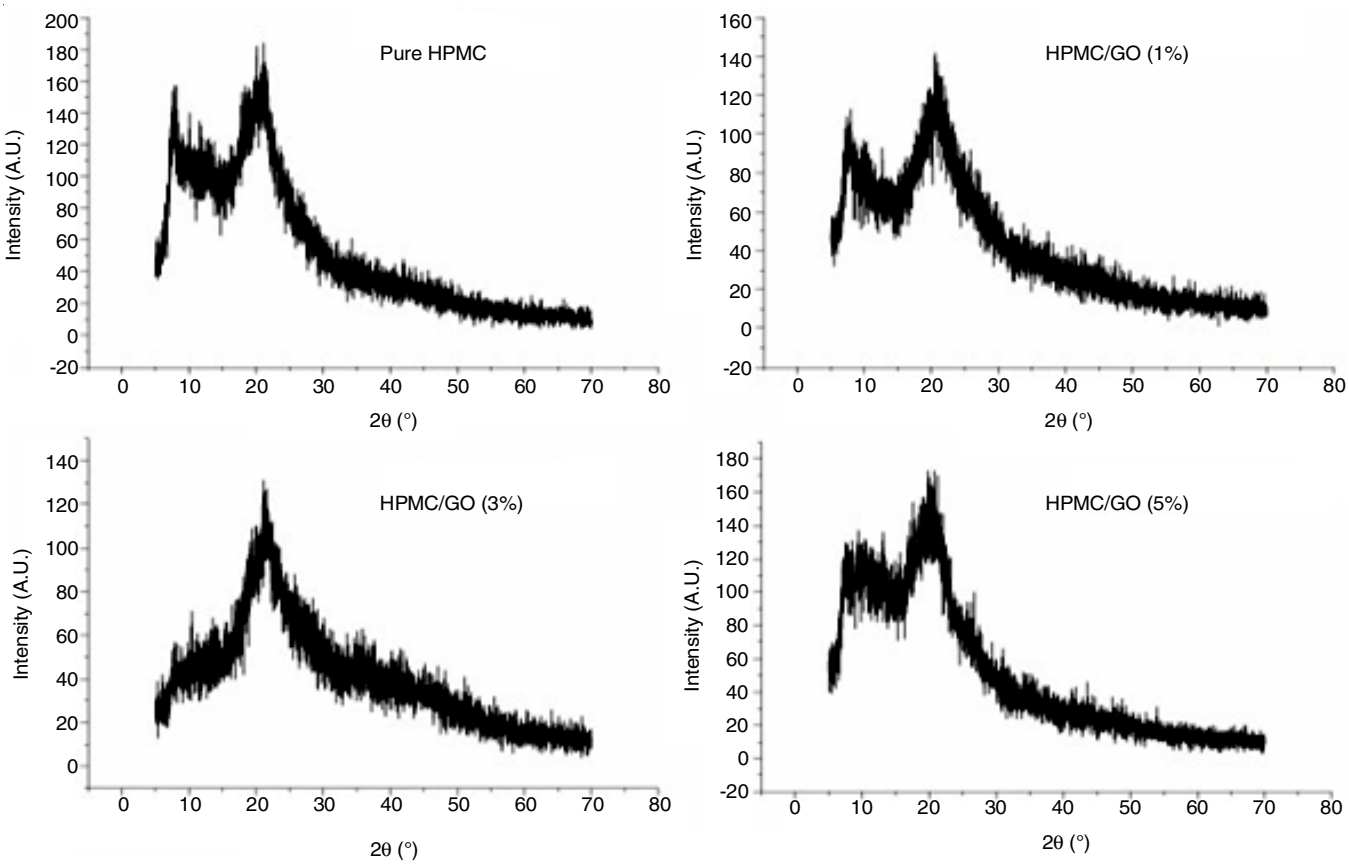

Fig. 1. XRD analysis data of HPMC/GO nanocomposite films

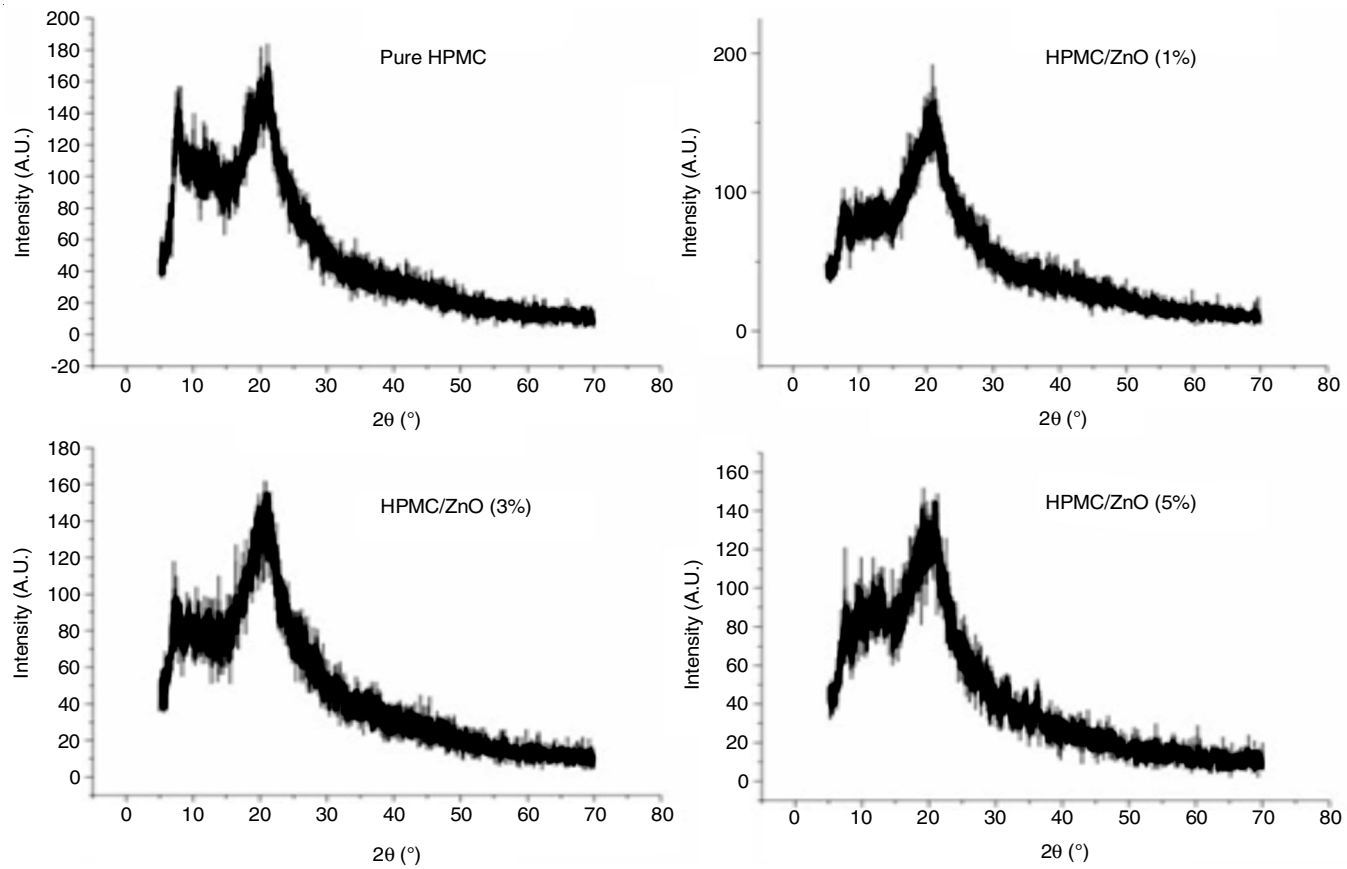

Fig. 2. XRD analysis data of HPMC/ZnO nanocomposite films

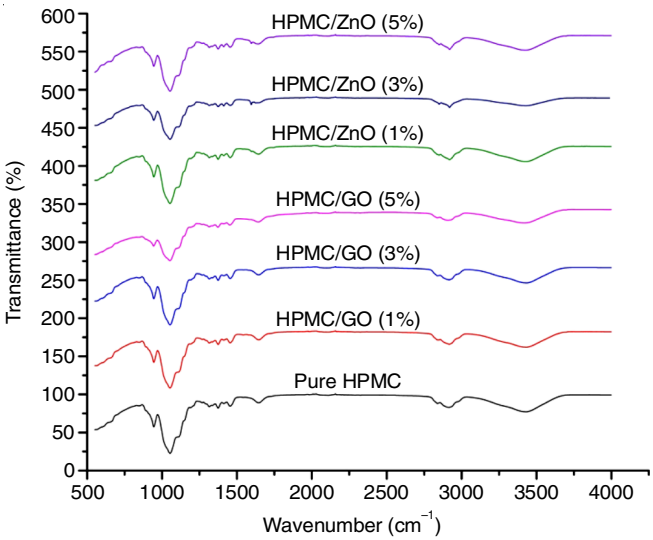

Fig. 3. FTIR spectrums of HPMC pure, HPMC/GO and HPMC/ZnO nanocomposite films

Thermal studies: In the presence of GO, the thermal stability of HPMC is increased, since GO and ZnO itself have strong thermal stability. It is visible that with the incorporation of GO, the thermal decomposition of pure HPMC moves towards higher temperatures (Fig. 4b-d).

The thermograms of nanocomposite films of HPMC/ZnO are shown in Fig. 4e-g, which indicated that in three steps, HPMC films demonstrate the decomposition. The key disintegration process of HPMC started at a temperature significantly below 100 ºC and increased to 150 ºC, due to the presence of moisture in the context. The subsequent degradation of polymer chains appear in the temperature range 150-350 ºC. For those HPMC/ZnO nanocomposite samples, the second weight reductions (major weight reductions) were observed in the region 240-370 ºC and can lead to the structural decomposition of the polymer nanocomposites [34]. However, as the nanoparticle dosage increased, the rate of thermal decomposition reaction of the samples decreases, but HPMC/ZnO nanocomposites are much more thermally stable relative to pure samples.

The degree of weight reduction of HPMC/GO and HPMC/ZnO nanocomposite films at various temperatures are shown in Table-1. At the composition of 5% addition of ZnO nanoparticles, the thermal stability varies to a decrease level, which may be due to the agglomerization of ZnO nanoparticles in the HPMC matrix. From the data, it is evident that the thermal stability of the HPMC polymer increases with addition of ZnO and GO nanoparticles.

Fig. 5a-d shows the DSC thermograms of HPMC and HPMC/GO nanocomposite films. The HPMC pure film transition temperature (T_g) was 78.99 ºC. The T_g of both polymer nanocomp-

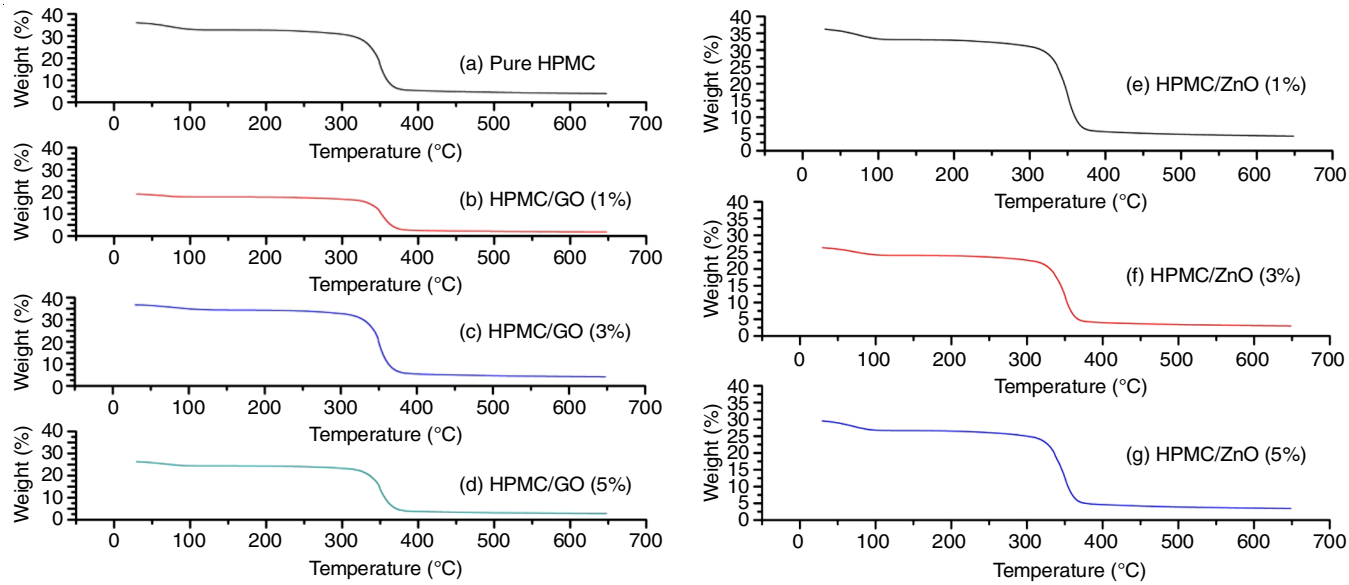

Fig. 4. TGA analysis spectra of Pure HPMC, HPMC/GO and HPMC/ZnO

TABLE-1
PERCENTAGE OF WEIGHT REDUCTION OF PURE HPMC AND HPMC COMPOSITES

Sample code	Percentage of weight loss at various temperature						
	100 °C	200 °C	300 °C	400 °C	500 °C	600 °C	Residue
Pure HPMC	8.39	9.45	14.63	85.45	87.54	88.77	3.89
HPMC/GO (1%)	7.01	7.52	12.66	85.39	87.50	88.66	1.86
HPMC/GO (3%)	4.96	6.77	11.06	85.32	87.41	88.50	4.09
HPMC/GO (5%)	7.06	7.79	11.59	85.81	87.86	88.98	2.80
HPMC/ZnO (1%)	8.05	9.19	14.33	84.40	86.50	87.57	4.37
HPMC/ZnO (3%)	8.09	9.18	14.30	84.85	87.05	88.17	3.01
HPMC/ZnO (5%)	9.43	10.42	15.60	84.44	86.83	87.97	3.43

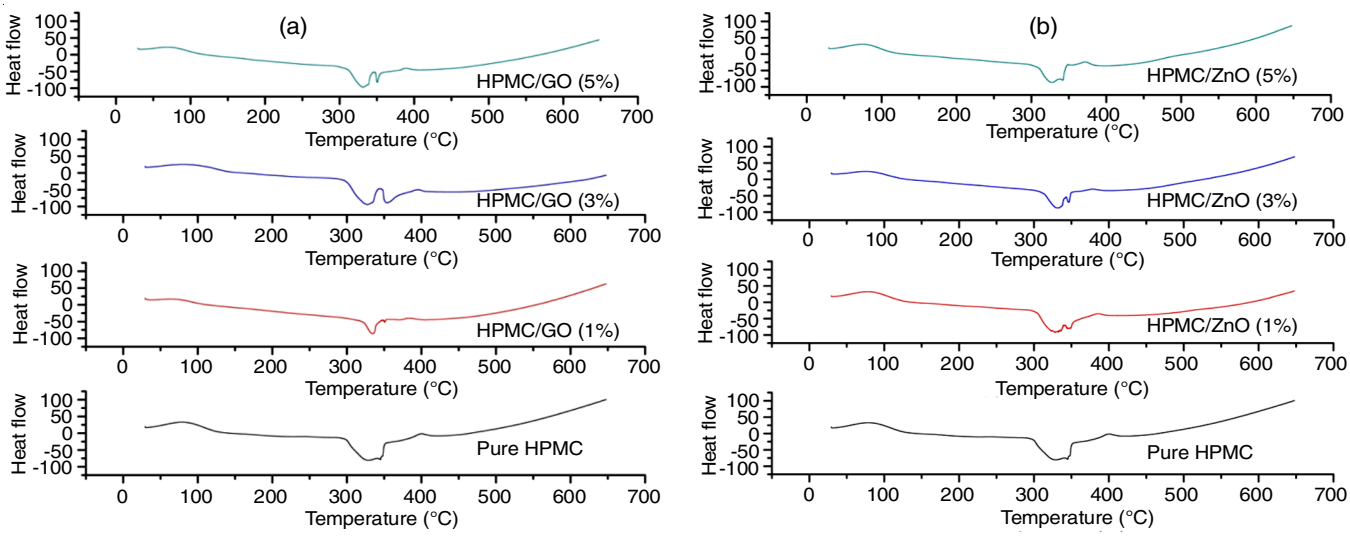

Fig. 5. DSC spectra of HPMC/GO (a) and HPMC/ZnO (b)

osite films decreases as the progress of the nanofillers rate builds up. The T_g of HPMC matrix decreases to < 70 ºC with the addition of 5 wt% of GO nanoparticle. By incorporating the GO and ZnO nanoparticles (Fig. 5e-g), the crystallinity of the polymer network increases, resulting to reduction in the transition temperature (T_g).

The mechanical properties *viz*. Young modulus, elongation at break and tensile strength for HPMC/ GO and HPMC/ZnO films were also evaluated. The films of pure HPMC showed the best medium of tensile strength and also revealed the elongation′s highest values (Table-2). The Young module is a parameter characterizing a material′s rigidity. In addition, it provides the hardness or resistance to elastic deformation in which this material offers. Higher the value of Young module in polymer will reflect with higher the deformation resistance and rigidity.

TABLE-2
MECHANICAL PROPERTIES OF PURE HPMC AND HPMC NANOCOMPOSITES

Sample code	Young's modulus (MPa)	Elongation at break (%)	Tensile strength (Mpa)
Pure HPMC	374.43	99.82	13.23
HPMC/GO (1%)	290.34	9.94	11.36
HPMC/GO (3%)	322.05	9.86	8.65
HPMC/GO (5%)	467.55	9.96	5.64
HPMC/ZnO (1%)	346.74	15.68	10.11
HPMC/ZnO (3%)	303.72	9.80	6.47
HPMC/ZnO (5%)	376.62	9.80	3.74

Both tensile strength and elongation at break decreased by raising the GO and ZnO content in the control HPMC films. The Young modulus shows a slight increasing behaviour, which goes on 5% addition of nanoparticles. The reason for the lowering mechanical properties tendency was due to non-alignment and non-strong surface interaction of nanoparticles.

The band gap and the form of electronic transitions were recorded in order to study the optical properties of the HPMC based nanocomposites. If a semiconductor absorbs energy photons greater than that of the semiconductor gap, an electron is moved from its valence band to the conduction band, there is an immediate rise in the material absorption to the wavelength corresponding to that same energy gap of the band. Fig. 6 shows the UV spectra of HPMC/GO and HPMC/ZnO.

From Table-3, it is clear that the band gap values are almost identical, ranging between 4.1 and 4.28 eV, and still lower than the pure samples. As a result, the values obtained indicate a dependency on the sample composition. It is possible that the differences are due to changes in the HPMC ions available for conduction per unit length, as well as changes in molecular structure caused by doping concentration.

TABLE-3
OPTICAL BAND GAP ENERGIES OF HPMC AND HPMC COMPOSITES

Sample code	Band gap (eV)
Pure HPMC	4.28
HPMC/GO (1%)	4.25
HPMC/GO (3%)	4.21
HPMC/GO (5%)	4.10
HPMC/ZnO (1%)	4.28
HPMC/ZnO (3%)	4.27
HPMC/ZnO (5%)	4.14

Conclusion

In summary, graphene oxide was synthesized by modified Hummers method and zinc oxide by using precipitation method. The nanoparticles were incorporated in HPMC matrix with different weight ratio to produce the HPMC based polymer nanocomposite films. The XRD and FTIR studies confirmed the presence of nanoparticles and also the nature of polymer. There was an increase in the thermal stability and optical characteristics of the composites with the increased loading of nanoparticles. The optical band gap was decreased on the polymer by the sequential addition of nanoparticles, which indicated that the polymer has the potential ability of being conductive in compare with pure HPMC biopolymer. The transition temperature (T_g) of the HPMC polymer decreases with increasing percentage of GO and ZnO nanoparticles, which was due to

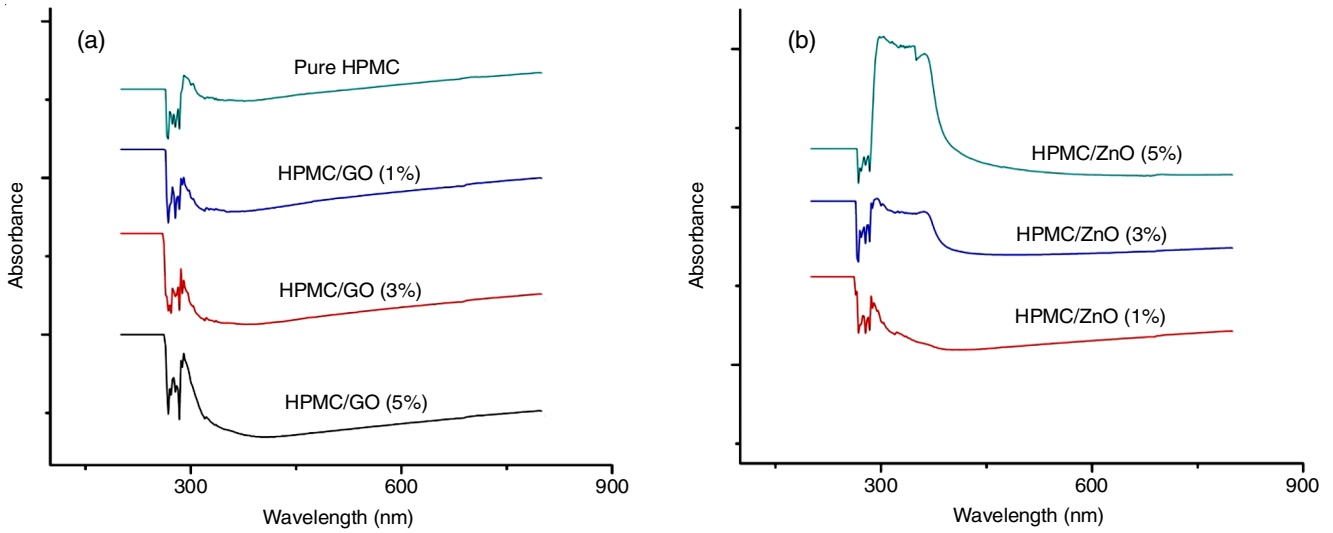

Fig. 6. UV spectra of HPMC/GO (a) and HPMC/ZnO (b)

the increased crystalline nature of the polymer. The weak interfacial interaction and non-uniformity of both GO and ZnO nanoparticles results the reduced mechanical properties.

CONFLICT OF INTEREST

The authors declare that there is no conflict of interests regarding the publication of this article.

REFERENCES

1. K. Müller, E. Bugnicourt, M. Latorre, M. Jorda, Y.E. Sanz, J.M. Lagaron, O. Miesbauer, A. Bianchin, S. Hankin, U. Bölz, G. Pérez, M. Jesdinszki, M. Lindner, Z. Scheuerer, S. Castelló and M. Schmid, *Nanomaterials*, **7**, 74 (2017); https://doi.org/10.3390/nano7040074
2. A. Sharma and P.S. Kumar, *Nanosci. Nanotechnol.*, **2**, 82 (2012); https://doi.org/10.5923/j.nn.20120203.07
3. S. Chandrasekaran, G. Faiella, L.A.S.D.A. Prado, F. Tölle, R. Mülhaupt and K. Schulte, *Composites A Appl. Sci. Manuf.*, **49**, 51 (2013); https://doi.org/10.1016/j.compositesa.2013.02.008
4. M.B.R. e Silva, M.I.B.Tavares, E.O. da Silva and R.P.C. Neto, *Polym. Test.*, **32**, 165 (2013); https://doi.org/10.1016/j.polymertesting.2012.09.006
5. M.I.B. Tavares, R.F. Nogueira, R.A. Silva San Gil, M. Preto, E.O. Silva, M.B.R e Silva and E. Miguez, *Polym. Test.*, **26**, 1100 (2007); https://doi.org/10.1016/j.polymertesting.2007.07.012
6. A. Kausar, *J. Plast. Film Sheet.*, **36**, 94 (2020); https://doi.org/10.1177/8756087919849459
7. S. Li, M.M. Lin, M.S. Toprak, D.K. Kim and M. Muhammed, *Nano Rev.*, **1**, 5214 (2010); https://doi.org/10.3402/nano.v1i0.5214
8. P.S.R.C.D. Silva and M.I.B. Tavares, *Mater. Res.*, **18**, 191 (2015); https://doi.org/10.1590/1516-1439.307314
9 F.A. dos Santos and M.I. Bruno Tavares, *Polym. Test.*, **47**, 92 (2015); https://doi.org/10.1016/j.polymertesting.2015.08.008
10. G. Kickelbick, Hybrid Materials: Synthesis, Characterization and Applications, John Wiley & Sons, p. 516 (2007).
11. M.S.S.B. Monteiro, C.L. Rodrigues, R.P. Neto and M.I.B. Tavares, *J. Nanosci. Nanotechnol.*, **12**, 7307 (2012); https://doi.org/10.1166/jnn.2012.6431
12. A.C.S. Valentim, M.I.B. Tavares and E.O. da Silva, *J. Nanosci. Nanotechnol.*, **13**, 4427 (2013); https://doi.org/10.1166/jnn.2013.7162
13. I.L. Soares, J.P. Chimanowsky, L. Luetkmeyer, E.O.D. Silva, D.D.H.S. Souza and M.I.B. Tavares, *J. Nanosci. Nanotechnol.*, **15**, 5723 (2015); https://doi.org/10.1166/jnn.2015.10041
14. A.S. Almeida, M.I.B. Tavares, E.O. Silva, R.P.C. Neto and L.A. Moreira, *Polym. Test.*, **31**, 267 (2012); https://doi.org/10.1016/j.polymertesting.2011.11.005
15. M.R. de Moura, F.A. Aouada, R.J. Avena-Bustillos, T.H. McHugh, J.M. Krochta and L.H.C. Mattoso, *J. Food Eng.*, **92**, 448 (2009); https://doi.org/10.1016/j.jfoodeng.2008.12.015
16. T.G. Smijs and S. Pavel, *Nanotechnol. Sci. Appl.*, **4**, 95 (2011); https://doi.org/10.2147/NSA.S19419
17. J.A. Ruszkiewicz, A. Pinkas, B. Ferrer, T.V. Peres, A. Tsatsakis and M. Aschner, *Toxicol. Rep.*, **4**, 245 (2017); https://doi.org/10.1016/j.toxrep.2017.05.006
18. R.T.R. Kumar, E. McGlynn, C. McLoughlin, S. Chakrabarti, R.C. Smith, J.D. Carey, J.P. Mosnier and M.O. Henry, *Nanotechnology*, **18**, 215704 (2007); https://doi.org/10.1088/0957-4484/18/21/215704
19. A. Kolodziejczak-Radzimska and T. Jesionowski, *Materials*, **7**, 2833 (2014); https://doi.org/10.3390/ma7042833
20. S. Sahoo, M. Maiti, A. Ganguly, J.J. George and A.K. Bhowmick, *J. Appl. Polym. Sci.*, **105**, 2407 (2007); https://doi.org/10.1002/app.26296
21. N. Li, W. Cheng, K. Ren, F. Luo, K. Wang and Q. Fu, *Chin. J. Polym. Sci.*, **31**, 98 (2013); https://doi.org/10.1007/s10118-013-1204-0
22. L. Lin, H. Deng, X. Gao, S. Zhang, E. Bilotti, T. Peijs and Q. Fu, *Polym. Int.*, **62**, 134 (2013); https://doi.org/10.1002/pi.4291
23. R. Bissessur and S.F. Scully, *Solid State Ion.*, **178**, 877 (2007); https://doi.org/10.1016/j.ssi.2007.02.030
24. S.M. Zhang, L. Lin, H. Deng, X. Gao, E. Bilotti, T. Peijs and Q. Fu, *Express Polym. Lett.*, **6**, 159 (2012); https://doi.org/10.3144/expresspolymlett.2012.17
25. A. Okada and A. Usuki, *Macrmol. Mater. Eng.*, **291**, 1449 (2006); https://doi.org/10.1002/mame.200600260
26. Y. Kojima, A. Usuki, M. Kawasumi, A. Okada, Y. Fukushima, T. Kurauchi and O. Kamigaito, *J. Mater. Res.*, **8**, 1185 (1993); https://doi.org/10.1557/JMR.1993.1185
27. S.N. Alam, N. Sharma and L. Kumar, *Graphene*, **6**, 1 (2017); https://doi.org/10.4236/graphene.2017.61001
28. S. Gahlot, P.P. Sharma, H. Gupta, V. Kulshrestha and P.K. Jha, *RSC Adv.*, **4**, 24662 (2014); https://doi.org/10.1039/C4RA02216E
29. Y. Sakata, S. Shiraishi and M. Otsuka, *Int. J. Pharm.*, **317**, 120 (2006); https://doi.org/10.1016/j.ijpharm.2006.02.058
30. R.M. Silverstein and F.X. Webster, Spectrometric Identification of Compounds, Wiley: New York, p. 71 (2002).
31. M. Govindarajan, S. Periandy and K. Ganesan, *E-J. Chem.*, **7**, 457 (2010); https://doi.org/10.1155/2010/702587
32. G.I. Titelman, V. Gelman, S. Bron, R.L. Khalfin, Y. Cohen and H. Bianco-Peled, *Carbon*, **43**, 641 (2005); https://doi.org/10.1016/j.carbon.2004.10.035
33. Y. Si and E.T. Samulski, *Nano Lett.*, **8**, 1679 (2008); https://doi.org/10.1021/nl080604h
34. E. Arkis and D. Balkose, *Polym. Degrad. Stab.*, **88**, 46 (2005); https://doi.org/10.1016/j.polymdegradstab.2004.02.021